This article was downloaded by: [UQ Library]
On: 04 January 2015, At: 17:11
Publisher: Taylor & Francis
Informa Ltd Registered in England and Wales Registered Number: 1072954 Registered office: Mortimer House, 37-41 Mortimer Street, London W1T 3JH, UK

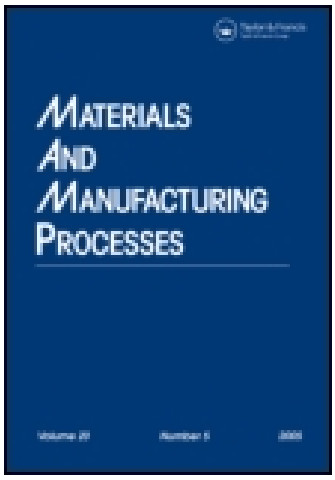

Materials and Manufacturing Processes
Publication details, including instructions for authors and subscription information:
http://www.tandfonline.com/loi/lmmp20

Simulation and Experimental Observations of Effect of Different Contact Interfaces on the Incremental Sheet Forming Process

Yanle Li [a] , Zhaobing Liu [a] , W.J.T.(Bill) Daniel [a] & P. A. Meehan [a]
[a] School of Mechanical & Mining Engineering , The University of Queensland , St Lucia , Brisbane , Australia
Accepted author version posted online: 29 Oct 2013.Published online: 04 Mar 2014.

Click for updates

To cite this article: Yanle Li , Zhaobing Liu , W.J.T.(Bill) Daniel & P. A. Meehan (2014) Simulation and Experimental Observations of Effect of Different Contact Interfaces on the Incremental Sheet Forming Process, Materials and Manufacturing Processes, 29:2, 121-128, DOI: 10.1080/10426914.2013.822977

To link to this article: http://dx.doi.org/10.1080/10426914.2013.822977

PLEASE SCROLL DOWN FOR ARTICLE

Taylor & Francis makes every effort to ensure the accuracy of all the information (the "Content") contained in the publications on our platform. However, Taylor & Francis, our agents, and our licensors make no representations or warranties whatsoever as to the accuracy, completeness, or suitability for any purpose of the Content. Any opinions and views expressed in this publication are the opinions and views of the authors, and are not the views of or endorsed by Taylor & Francis. The accuracy of the Content should not be relied upon and should be independently verified with primary sources of information. Taylor and Francis shall not be liable for any losses, actions, claims, proceedings, demands, costs, expenses, damages, and other liabilities whatsoever or howsoever caused arising directly or indirectly in connection with, in relation to or arising out of the use of the Content.

This article may be used for research, teaching, and private study purposes. Any substantial or systematic reproduction, redistribution, reselling, loan, sub-licensing, systematic supply, or distribution in any form to anyone is expressly forbidden. Terms & Conditions of access and use can be found at http://www.tandfonline.com/page/terms-and-conditions

Materials and Manufacturing Processes, 29: 121–128, 2014
Copyright © Taylor & Francis Group, LLC
ISSN: 1042-6914 print/1532-2475 online
DOI: 10.1080/10426914.2013.822977

Taylor & Francis
Taylor & Francis Group

Simulation and Experimental Observations of Effect of Different Contact Interfaces on the Incremental Sheet Forming Process

YANLE LI, ZHAOBING LIU, W.J.T. (BILL) DANIEL, AND P.A. MEEHAN

School of Mechanical & Mining Engineering, The University of Queensland, St Lucia, Brisbane, Australia

Incremental sheet forming (ISF) is a promising forming process perfectly suitable for manufacturing customized products with large plastic deformation by using a simple moving tool. Up to now, however, the effects of contact conditions at the sheet interface are not well understood. The aim of this work is to study the effect of tool type and size on the formability and surface integrity during the forming process. Experimental tests were carried out on aluminum sheets of 7075-O to create a straight groove with four different tools (ϕ 30, ϕ 25.4, ϕ 20 and ϕ 10 mm). One tool tip was fitted with a roller ball (ϕ 25.4 mm) while the other three were sliding tips. The contact force, friction and failure depth were evaluated. A finite element (FE) model of the process was set up in an explicit code LS-DYNA and the strain behavior and thickness distribution with different tools were evaluated and compared with the experimental results. This study provides important insights into the relatively high formability observed in the ISF process. Microscopic observations of the surface topography revealed that a rolling tool tip produced better surface integrity as compared with a sliding tool tip, wherein, distinct scratch patterns in the tool traverse direction were evident.

Keywords Deformation; Forces; Forming; Strain; Stresses.

Downloaded by [UQ Library] at 17:11 04 January 2015

INTRODUCTION

Incremental sheet forming (ISF) is a promising manufacturing process in which flat metal sheets are gradually formed into 3D shapes using a generic tool stylus only. By using this process, useable parts can be formed directly from computer-aided design (CAD) data with a minimum of specialized tooling; therefore, it has economic benefits for rapid prototyping production and for small quantity applications [1–3].

Over recent years, different kinds of studies have been conducted [2, 4–9] with emphasis on understanding, assessing and improving the formability in this forming process. Among them, straight groove tests have been performed by Kim and Park [10] and suggested as an appropriate method to evaluate the effects of process parameters on the formability for aluminum sheet. In this forming test, two characteristics of deformation can be achieved [10]. One is the deformation condition. Biaxial stretching deformation takes place at the starting and ending points of the straight line when the tool moves horizontally. As the forming depth increases, the deformation turns more into biaxial stretching. On the contrary, plane-strain stretching deformation occurs between the starting and ending points. Another important characteristic of ISF is the higher formability achieved compared with other conventional sheet forming processes. As for deformation mechanics of ISF, stretching rather than vertical shearing appears to be the dominant mode of deformation in ISF according to recent published work by Silva [11] and Allwood [12]. Failure mechanics in ISF [13] were revisited recently and a much deeper insight on the influence of tool radius led to the proposal of a new understanding and assessing on formability limits and formation process of fracture. Minutolo [14], working on force analysis in the groove test, found that using a tool with a bigger diameter and higher drawing depth, higher forming forces and a different typology of failure can be observed. However, comparison between the results using ball (rolling) and hemispherical (sliding) tools were not conducted in this article. Kim [10] concluded that the ball tool is more effective than the hemispherical head tool in terms of formability by simply judging the value of $(\varepsilon_{major}+\varepsilon_{minor})$ [4] after deformation, without comparing the failure depth of two kinds of tools. Durante [15] and Hussain [16], working on the effect of tool/sheet contact conditions on the surface finish of the product, found that the lowest levels of surface roughness were obtained with sphere/sheet contact. Still, surface topography of the forming surface needs to be studied to deepen the knowledge in the effect of different contact conditions on this innovative sheet forming process.

In the present paper, the test to form a straight groove has been carried out and the effect of tool size, tool type and friction between tool and sheet was investigated. One of the few state-of-the-art ISF machines designed by Amino Corporation that allows mold based forming for a maximum

Received February 22, 2013; Accepted June 26, 2013

Address correspondence to Yanle Li, School of Mechanical & Mining Engineering, The University of Queensland, St Lucia, Brisbane, QLD 4072, Australia; E-mail: yanle.li@uq.edu.au.

Color versions of one or more of the figures in the article can be found online at www.tandfonline.com/lmmp.

size 2100 mm × 1450 mm × 550 mm with greater control and quality was used to conduct the forming process. In terms of the sliding conditions, three hemispherical head tools, 30 mm, 20 mm and 10 mm in diameter, have been used. From these experimental tests, the influence of tool sizes on the surface topography and on the value of the failure can be analyzed and revealed. In addition, some failure cases during the process are analyzed to provide experimental evidence on fracture forming limits. A FE model has also been created and utilized to analyze the strain behavior for better understanding the deformation mechanics.

Experimentation and simulation methods

Experiment Setup

The groove forming tests have been performed on a state-of-the-art machine designed dedicated for the ISF process by Amino Corporation which can be numerical controlled by a controller provided by FANUC corporation. Fig. 1 shows a photograph of an experimental test.

Two types of tools; a ball tool and hemispherical head tool as pictured in Fig. 2, have been used in the experiment to produce four different contact interfaces between tool and workpiece. Among them, a ball, with a diameter of 25.4 mm, attached to the end of the ball tool can rotate freely. For the hemispherical tool, the tip is tungsten carbide and the body is made of K110 steel which was hardened and tempered to HRC60. The material used in the present study was aluminum 7075-O sheet of 300 mm × 300 mm in size and 1.016 mm in thickness. Alloy 7075 was one of the most successful Al–Zn–Mg–Cu alloys with high strength and good stress-corrosion cracking resistance and has been widely used for aerospace applications.

In the groove test, metal sheets were fixed along their edges in a special designed frame which mounted on the forming table of the machine; the tool moved back and forth

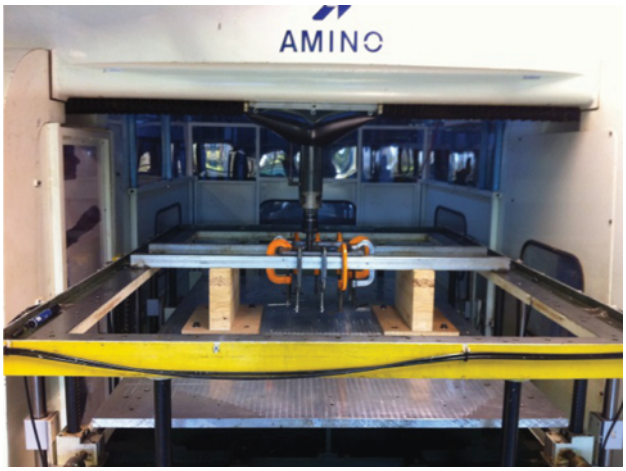

Figure 1.—Incremental sheet forming on Amino machine.

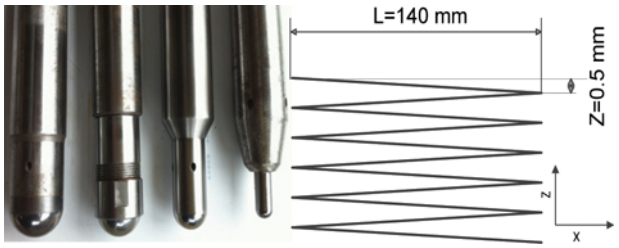

Figure 2.—Four different tools and tool path that were utilized in the experiments.

along a 140 mm long straight path (shown in Fig. 2) with a gradual step down of 0.5 mm in vertical position until a crack was observed. For every test, a feed rate of 1000 mm/min has been set out and a lubricant has been sprayed on the plate to reduce the friction coefficient between tool and sheet surfaces. More detailed configurations for the experimental parameters can be found in Table 1.

Finite Element (FE) Model

By comparing different simulation package and performance [17, 18], DYNA3D, a dynamic explicit FE code, is chosen to simulate the drawing process. It can accurately solve dynamic problems which have 3D elastic–plastic large deformation using explicit time integration. Due to the complexity of the ISF simulation, mass scaling and increasing working speed was essential to reduce computing time with insignificant influence on the simulation results.

The general geometry of the sheet is square with dimension 300 mm × 300 mm and it is meshed into 1.5 mm × 1.5 mm elements which are shown in Fig. 3 (only half of the sheet is presented). To simulate the boundary conditions in the forming process, nodes in all edges are constrained with both displacement and rotation in all degrees of freedom. In the FE model, forming tools are considered as rigid bodies and their boundary conditions that should be followed during the process are given by the path shown in Fig. 2. In the presented FE model, the sheet behavior is assumed to be isotropic and the plastic property is modeled by means of a power law expression. This expression considered the material hardening with an exponential dependence on strain but neglected the effect of both temperature and strain rate to simplify the model. Material parameters were obtained from the work by M. Durante [19] which are shown in Table 2. From our

Table 1.—Experimental parameters design for groove test.

Part No.	Tool size (mm)	Sheet thickness (mm)	Groove length (mm)	Speed (mm/min)
1	30	1.016	140	1000
2	20	1.016	140	1000
3	10	1.016	140	1000
4	25.4(ball)	1.016	140	1000

Downloaded by [UQ Library] at 17:11 04 January 2015

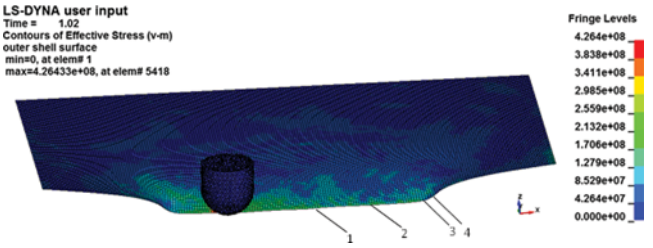

FIGURE 3.—FE model of the ISF process in LS-DYNA. Reference elements 1–4 marked.

experimental work, the friction at the contact surface between tool head and sheet has been assessed and analyzed with a value of 0.18. This value has been used in this FE model (see Fig. 4).

EXPERIMENTATION AND SIMULATION RESULTS

Force Measurement

To better understand the contact mechanics and predict the occurrence of failure, the forces between tool and workpiece have been measured continuously over time during the process. There are several ways to capture the forming force, such as the cantilever sensor designed by Jeswiet [20] and force dynamometer used by Duflou [21]. In the present work, three full Wheatstone bridges have been designed and mounted on the 30 mm hemispherical tool. Each bridge is configured by four strain gauges and designed to measure one of the three orthogonal forces: two bending directions, and one axial direction. Before taking any measurement, the strain gauges were calibrated twice in all three directions by applying a known force to get an accurate result. The calibrated system shows a rather linear relation between strain and output voltage.

The forces measured with this system shown in Fig. 4 are for a 1.016 mm thick 7075-O aluminum sheet. In this test, a groove was formed until it was 25 mm deep when fracture of the aluminum sheet occurred. It can be seen that both vertical and horizontal components experience a sharper increase at the end of each travel and the maximum forces encountered are around $Fv = 2700$ N in the vertical direction and $F_h = 1800$ N in the horizontal direction. These sharper increases are likely due to three main reasons; the increase of the contact area at the end of the groove, the dynamic impact of the side wall and also the large acceleration of the forming tool caused by the sudden change of moving direction. For the steps (vertical depth from 15 mm to 25 mm where failure occurs) which were presented in Fig. 4, only a slight increase from 800 N to 1000 N for the vertical and from 150 N to 200 N for the horizontal component can be found for the nearly steady trend recorded in the middle of each travel. Evaluation of friction coefficients is conducted by calculating the absolute value of the ratios between horizontal and vertical components in the central area of the specimens, which has been widely used by Durante [19] and Hamilton [22]. According to Fig. 4, the absolute value of the ratios shows a slightly growing tendency in the middle area of the groove caused by the continual increase of the groove depth which requires more forces to stretch the sheet during each travel. An average value of 0.18 has been calculated as the average friction coefficient.

TABLE 2.—Mechanical properties for 7075-O aluminum sheet.

Parameters	Value
Sheet thickness (mm)	1.016
Young's modulus (GPa)	75
Yield strength (MPa)	100
Ultimate tensile strength (MPa)	200
Poisson's ratio	0.33
Plastic property	$\sigma = 330\varepsilon^{0.19}$

Failure Depth

Hemispherical head tools of three sizes were used: 10, 20 and 30 mm in diameter. We can obviously see from Fig. 5 that the failure depth is higher with an increase in tool diameter. More specifically, cracking occurs when the forming depth was 16, 21.5 and 25 mm for the tool diameters of 10, 20 and 30 mm with rolling direction (RD), respectively. It is worth noting that all the cracks first occurred near the end of each travelling path: this is due to the fact that these are the regions where the highest amount of deformation, straining and thinning will take place. It appears that there are linear relations between these failure depths and tool diameters in the test coverage. It can be clearly concluded from the

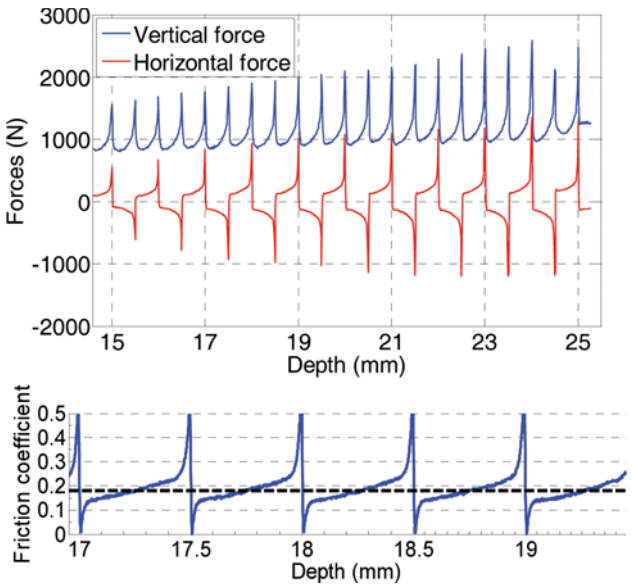

FIGURE 4.—Vertical and horizontal force with a tool of 30 mm in diameter and the absolute value of the ratios between two components.

Downloaded by [UQ Library] at 17:11 04 January 2015

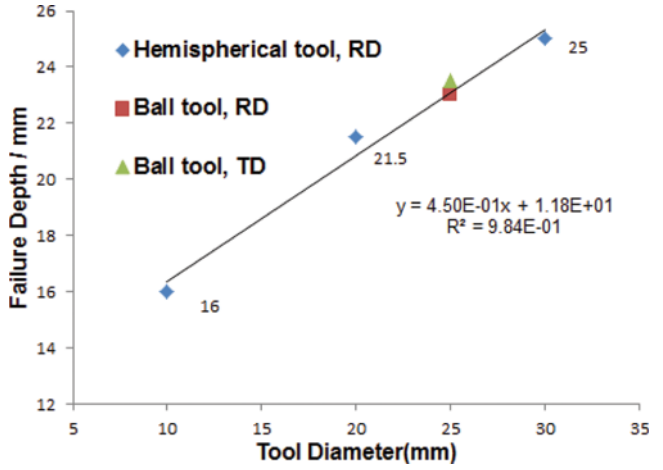

FIGURE 5.—Variations of failure depth of the groove test with tools different in diameter. (RD represents rolling direction and TD for transverse direction).

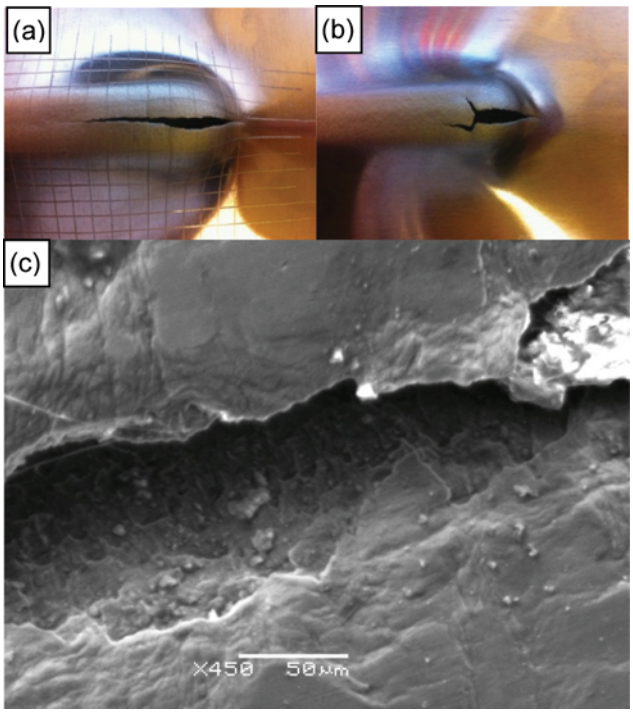

FIGURE 6.—Failure types of sheets formed with different tools. (a) Monodirectional; (b) bidirectional failure; (c) scanning electron micrograph of the onset of fracture and the cross section.

Downloaded by [UQ Library] at 17:11 04 January 2015

experimental results that the tool diameter should be chosen as large as possible to delay the fracture. These results are consistent with the technical literature [23] in that, with the decrease of the tool diameter, the plastic deformation area also descends but the strain level ascends. The higher level of stresses can explain the early failure with the smaller sized tools.

In terms of the ball tool with a diameter of 25.4 mm, two tests have been performed with the forming direction parallel to ball direction (RD) and transverse direction (TD). The failures of these grooves were recorded at 23 mm and 23.5 mm when the tool was moving along TD and RD, respectively. This phenomenon indicates that a small amount of plane-anisotropy results in the small difference of formability between two directions of the tool.

Figure 6 shows two different failure types at the end of the groove formed by 30 mm large ball tool (a) and hemispherical tool (b), respectively. By checking both macro (Fig. 6(a)) and micro (Fig. 6(c)) structure of the failure point, it is shown that plastic deformation develops by uniform thinning until fracture and in-plane stretching is the principal mode of deformation in this process.

Contact Forces, Strain Behavior and Thickness Distribution in FE Model

To validate the proposed FE model, the simulated contact forces were plotted and compared with experimental data which is shown in Fig. 7. In the FE model, both the tool and the sheet are modeled with the same parameters as in the experimental test (e.g. sheet thickness is 1.016 mm, tool diameter is 30 mm and groove length is 140 mm). From Fig. 7, the predicted forces both in vertical and horizontal components are in reasonable agreement with measured values, except that vertical forces are slightly overestimated and at the end points of the groove sharper force peaks were recorded in the experimental test. The deviation of the modeled and measured force results for the peak values may be due to two main aspects: (1) 7075-O aluminum alloy is strain-rate sensitive and in the case of strain-rate sensitive materials artificially increasing the working speed might adversely affect accuracy of predicted forming forces. In the current model, the forming speed is artificially increased by a time scaling factor of 16.8 to save computing time. (2) Model boundary conditions might not have corresponded to reality. Specifically, there may have been a small amount of sliding between metal sheets and the clamping frame that was not included in the model. It is also possible that dynamic impact of the side wall and acceleration of the forming tool have not been quite accurately modeled. These aspects should be further investigated for developing an accurate force prediction model. However, for the investigation of strain behavior and thickness distribution in this process, the predicted forming forces during the groove forming process are acceptable as conservative measures.

The strain behavior of the sheet was predicted by LS-DYNA. The results of the strain distribution can provide useful information to understand the trend of deformation. To compare the state of the strain for the tool diameter of 30 and 20 mm, the analysis were performed until the forming depth both reached 21 mm.

Figure 8 shows the major strain distribution in the middle of the groove along the longitude direction in which the value of the contacted surface and non-contacted are denoted by upper surface and lower surface, respectively. In this

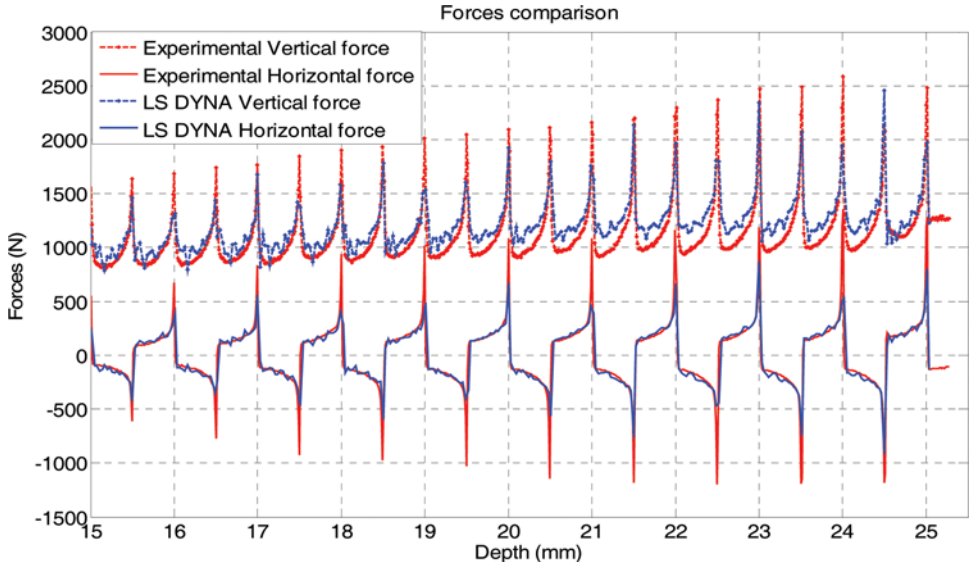

FIGURE 7.—Forces comparison between simulated and experimental results.

figure, the major strain is small in the middle and big at the end of the groove and the major strain on the lower surface is greater than that on the upper surface. It can also be noticed in Fig. 8 that the major strain with the 20 mm tool is greater than that with the tool diameter of 30 mm for both upper surface and lower surface. It suggests that the level of strain decreases as the tool size increases. This could be explained physically by the increase in the contact area and deformation zone. Since the forming limit of the sheet is restricted by the value of strain, earlier occurrence of failure using a smaller tool can be predicted.

To further study the strain behavior and the evolution of the groove, four elements at the bottom of the groove at different places have been selected to compare the strain evolution history in the forming process as shown in Figs. 3, 9 and 10. In the current coordinate system, the origin is defined at the center of the sheet and the tool is travelling along the X-axis from –70 mm to 70 mm while keeping Y as 0. The X-coordinate values of the four selected elements 1, 2, 3 and 4 are 0 mm, 35 mm, 64 mm and 70 mm, respectively (see Figs. 3 and 10). Figure 9 illustrates the strain evolution history of the four elements during the whole forming process which uses a tool with a diameter of 30 mm. It can be clearly noticed that the strain values of the elements (1 and 2) in the middle of the groove keep the same level at each step and the lowest strain values always take place at the very end of the groove (element 4). However, by checking the strain values of each element, it was found that the maximum effective strain occurs before the corner of the groove (element 3) with a distance of 6 mm. The FE modeling results can be confirmed by Fig. 6 which shows that the crack first occurs just prior to the end of the groove.

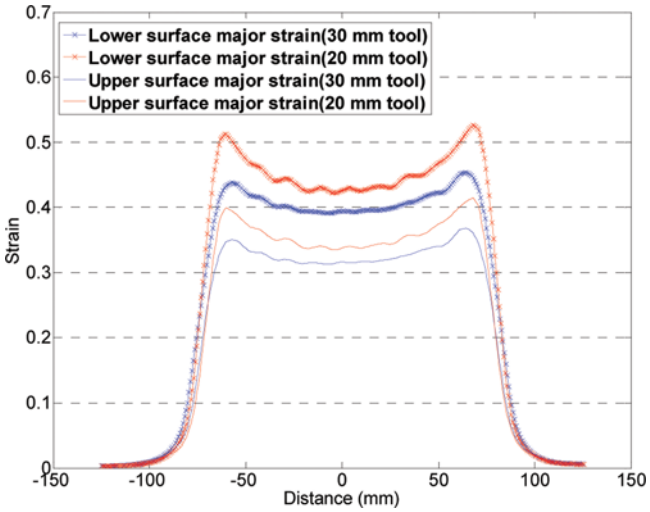

FIGURE 8.—Distributions of major strain predicted by LS-DYNA with different size tools at the depth of 21 mm.

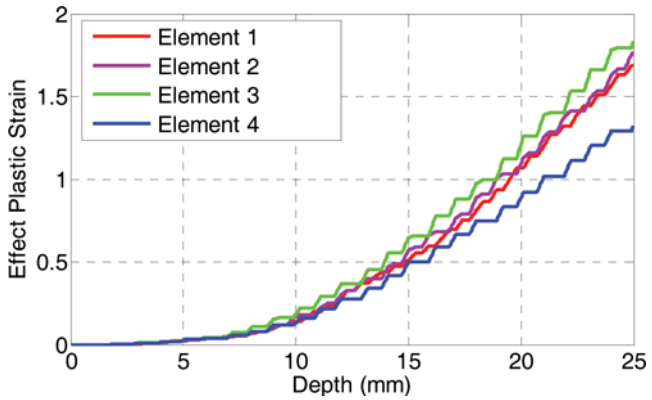

FIGURE 9.—Effective plastic strain evolution of four elements in a groove forming process with 30 mm tool.

Downloaded by [UQ Library] at 17:11 04 January 2015

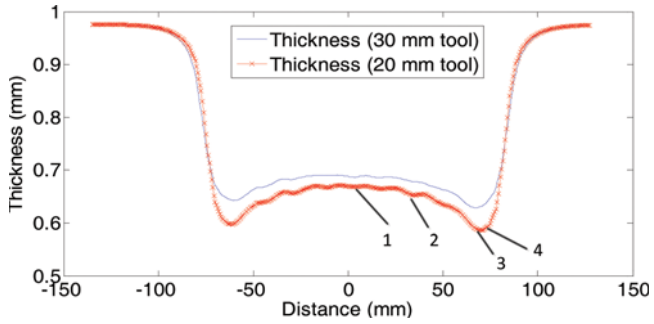

FIGURE 10.—Thickness distributions predicted by LS-DYNA with different size tools. Reference elements 1–4 marked.

Based on the assumption that the metal sheet is incompressible, the large deformation takes place by thinning the sheet. As a result, the thickness distribution is a critical factor to assess the formability and feasibility of a process. The thickness distribution with tools of 30 and 20 mm in diameter are simulated by LS-DYNA and shown in Figure 10. It can be obviously seen that the thickness is greater in the middle and smaller at the ends of the path which can explain why the failure always occurs at the end of the groove. At the same forming depth, the thickness of the groove formed by the 20 mm tool is thinner than that formed by the 30 mm tool, which suggests that failure should occur earlier for the smaller tool. These predicted FE strain and thickness analysis results are well corroborated by the experimental tests performed in the present work.

Surface Topography (SEM)

Figure 11 shows the aluminum sheet surface topography of the grooves produced by hemispherical (a) and ball tools (b) scanned by using JEOL6460 Scanning Electron Microscopy (SEM) with the supply power of 15 KV. The samples were cut into 2 cm squared for SEM observation and no other surface treatment was performed. Compared with sliding contact, the surface damage (striations) of the parts formed under rolling contact appears to be less. Fig. 11 also indicates that many small pits appear on the surface of the aluminum sheet formed with both hemispherical and ball tool. This appears to be due to the coating exfoliating [24] on the sheet.

The border zone between the touched and non-touched area formed by the ball tool are also captured by SEM (Fig. 12). Interesting differences between these two areas can be seen that the surface formed by the ball tool appears smoother than the initial unformed surface. To some extent, it appears that the rolling contact condition can improve the surface topography by flattening the rolling trace initially existing on the sheet surface. However, much more detailed examination should be taken to fully explain this phenomenon.

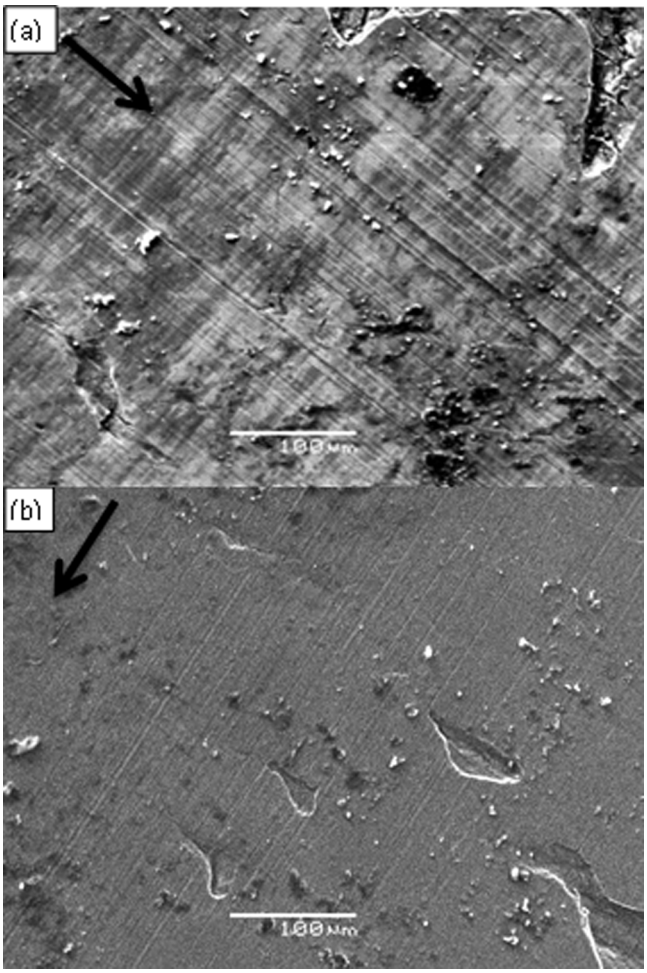

FIGURE 11.—Surface topography examined by SEM for sheets formed with different tools along the directions indicated by arrows: (a) hemispherical tool; (b) ball tool.

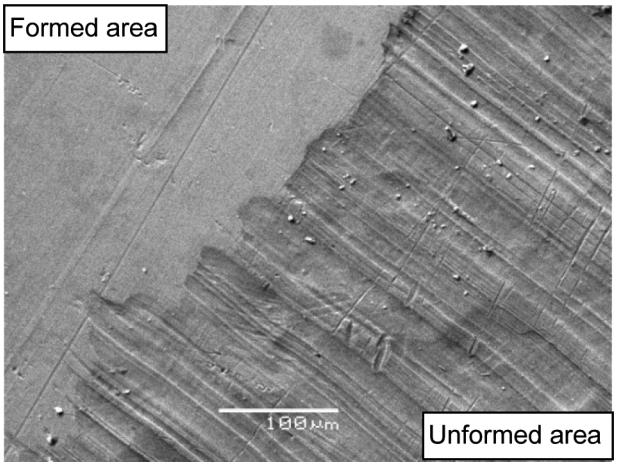

FIGURE 12.—Border zone of the contacted and non-contacted area with ball tool.

Downloaded by [UQ Library] at 17:11 04 January 2015

Downloaded by [UQ Library] at 17:11 04 January 2015

Conclusion

Forming forces have been measured by means of strain gauges and provide useful information to monitor and understand the forming process. Even though both vertical and horizontal forces present sharper increases at the end of each travel due to the increase of contact area and impact to the side wall, forces only show a slightly growing trend in the central area of the groove. This information proves that only localized deformation occurred in the process and thus it is possible to form large and complex shapes without higher forces required. By recording the forming depth using three different size tools, an obvious increasing trend in fracture depth was observed with the increase of tool diameter. Therefore, tool diameter should be selected as large as possible to improve formability with the constraints of geometrical complexity. Surface topography of parts formed by the hemispherical and ball tools has been scanned by SEM. The result shows that rolling contact condition causes much less local damage and scratching of the surface. FE analysis is an efficient way to determine the influence of different tool sizes on the strain behavior and thickness distribution, providing how different parameters affect the forming process.

To further compare the effect of contact types, the same size of hemispherical tool (25.4 mm) is being manufactured and would be utilized in future research. Surface roughness is another important parameter to evaluate the output quality of the process and should also be measured in the future.

Acknowledgments

The authors are grateful to Paul Bellette and Peter Bleakley, for their assistance of the initial setup of the experiment test. Revision of the manuscript provided by Dr Prasad Gudimetla is also greatly acknowledged.

Funding

This work is financed by Australian Research Council (ARC) Linkage project which collaborates with QMI Solutions. China Scholarship Council (CSC) is acknowledged for the scholarship support.

References

1. Jeswiet, J., et al., Asymmetric single point incremental forming of sheet metal. *Annals of CIRP—Manufacturing Technology* **2005**, *54*(2), 623–649.
2. Echrif, S.B.M.; Hrairi, M. Research and progress in incremental sheet forming processes. *Materials and Manufacturing Processes* **2011**, *26*(11), 1404–1414.
3. Leacock, A.G.; The future of sheet metal forming research. *Materials and Manufacturing Processes* **2012**, *27*(4), 366–369.
4. Iseki, H.; Kumon, H. Forming limit of incremental sheet metal stretch forming using spherical rollers. *The Japan Society for Technology of Plasticity* **1994**, *35*, 1336.
5. Kim, T.J.; Yang, D.Y. Improvement of formability for the incremental sheet metal forming process. *International Journal of Mechanical Sciences* **2000**, *42*(7), 1271–1286.
6. Sarraji, W.K.H.; Hussain, J.; Ren, W.-X. Experimental investigations on forming time in negative incremental sheet metal forming process. *Materials and Manufacturing Processes* **2011**, *27*(5), 499–506.
7. Hussain, G.; Gao, L.; Hayat, N. Forming parameters and forming defects in incremental forming of an aluminum sheet: correlation, empirical modeling, and optimization: Part A. *Materials and Manufacturing Processes* **2011**, *26*(12), 1546–1553.
8. Banabic, D.; Sester, M.; Influence of material models on the accuracy of the sheet forming simulation. *Materials and Manufacturing Processes* **2012**, *27*(3), 273–277.
9. Silva, M.B.; Martinho, T.M.; Martins, P.A.F. Incremental forming of hole-flanges in polymer sheets. *Materials and Manufacturing Processes* **2013**, *28*(3), 330–335.
10. Kim, Y.H.; Park, J.J. Effect of process parameters on formability in incremental forming of sheet metal. *Journal of Materials Processing Technology* **2002**, *130–131*, 42–46.
11. Silva, M.B., et al. Single-point incremental forming and formability-failure diagrams. *Journal of Strain Analysis for Engineering Design* **2008**, *43*(1), 15–35.
12. Allwood, J.; Shouler, D.; Tekkaya, A.E. The increased forming limits of incremental sheet forming processes. *Key Engineering Materials* **2007**, *344*, 621–628.
13. Silva, M.B., et al. Failure mechanisms in single-point incremental forming of metals. *The International Journal of Advanced Manufacturing Technology* **2011**, *56*(9), 893–903.
14. Minutolo, F.C., et al. Forces analysis in sheet incremental forming and comparison of experimental and simulation results. In *Intelligent Production Machines and Systems-2nd IPROMS Virtual Internationl Conference*, Cardiff, England, July 3–14, 2006.
15. Durante, M.; Formisano, A.; Langella, A. Observations on the influence of tool-sheet contact conditions on an incremental forming process. *Journal of Materials Engineering and Performance* **2011**, *20*(6), 941–946.
16. Hussain, G., et al. Guidelines for tool-size selection for single-point incremental forming of an aerospace alloy. *Materials and Manufacturing Processes* **2012**, *28*(3), 324–329.
17. Vafaeesefat, A. Finite element simulation for blank shape optimization in sheet metal forming. *Materials and Manufacturing Processes* **2011**, *26*(1), 93–98.
18. Cai, G.P.; Zhu, N.Y.; Wen, N. Stress analysis of sheet metal vibration incremental forming. In *Materials Processing Technologies, Pts 1 and 2*; Z.Y. Jiang, X.H. Liu, and J.L. Bu, Eds.; Trans Tech Publications Ltd: Stafa-Zurich, 2011; 166–170.
19. Durante, M., et al. The influence of tool rotation on an incremental forming process. *Journal of Materials Processing Tech* **2009**, *209*(9), 4621–4626.
20. Jeswiet, J.; Alexander Szekeres, J.R.D. Forces in single point and two point incremental forming. *Advanced Materials Research* **2005**, *6–8*, 449–456.
21. Duflou, J.R. Force measurements for single point incremental forming: an experimental study. *Advanced Materials Research* **2005**, *6–8*, 441–448.

22. Hamilton, K.A.S. Friction and external surface roughness in single point incremental forming: a study of surface friction, contact area and the 'orange peel' effect, 2010.
23. Carrino, L.; Giuliano, G.; Strano, M. The effect of the punch radius in dieless incremental forming. In *Intelligent Production Machines and Systems–2nd IPROMS Virtual International Conference*, Cardiff, England, July 3–14, 2006; 204–209.
24. Hou, Y.K., et al. Surface topography evolvement of galvanized steels in sheet metal forming. *Transactions of Nonferrous Metals Society of China* **2009**, *19*(2), 305–310.

Downloaded by [UQ Library] at 17:11 04 January 2015